ELSEVIER

www.elsevier.nl/locate/jphotobiol

J. Photochem. Photobiol. B: Biol. 54 (2000) 175–184

Journal of Photochemistry and Photobiology B:Biology

Chromosomes are target sites for photodynamic therapy as demonstrated by subcellular laser microirradiation

Hong Liang, Tuyen Do, Sanaz Kasravi, Parnaz Aurasteh, Andrea Nguyen, Andy Huang, Zifu Wang, Michael W. Berns *

Beckman Laser Institute and Medical Clinic, University of California, Irvine, Irvine, CA 92612, USA

Received 29 September 1999; accepted 17 January 2000

Abstract

The present investigation has been undertaken to examine the possibility that the cell nucleus, and specifically the genetic material, is a target site for photodynamic therapy. PTK_2 and Hep-2 cells are pretreated with a medium containing 15 μg/ml (0.09 mM) 5-aminolevulinic acid (ALA). Individual fluorescence images are recorded for each selected cell using a cooled charge-coupled device (CCD). A laser microbeam system generating 630 nm is used for subcellular-region irradiation of specific targets: chromosomes, the mitotic spindle, the perispindle region and the peripheral cytoplasm. Nuclei of interphase cells are also irradiated. Data comparing the sensitivities of the different subcellular microirradiation sites in ALA-treated mitotic cells demonstrate that under the irradiation conditions used, the chromosome is the most sensitive subcellular target followed by the perispindle region, the peripheral cytoplasm and spindle, and, lastly, the interphase nucleus.

Keywords: 5-Aminolevulinic acid (ALA); Photosensitizers; Photodynamic therapy (PDT); Fluorescence; Chromosomes; Nuclei; Laser microbeam irradiation

1. Introduction

Photodynamic therapy (PDT) is an accepted modality for the treatment of certain types of malignant tumors [1,2]. In addition, it is showing great promise in the treatment and management of a variety of non-malignant conditions such as dysfunctional uterine bleeding [3], macular degeneration [4,5], dermatological port-wine stains [6], psoriasis [7,8] and atherosclerosis [9,10].

Considerable research on the mechanisms of PDT has been conducted at the cellular, tissue and tumor levels. These studies have been on photochemical mechanisms of cell and tumor destruction, the structural and biochemical basis of cell and tumor destruction, as well as the uptake and binding of PDT agents at the cell and tumor levels [11].

Much of the in vitro cell work has involved sensitizer screening, uptake and binding studies, and electron microscope studies that examine the structural changes occurring as a result of PDT [11]. Of these, only a few have involved the exposure of specific subcellular target regions/organelles to light following treatment with the photosensitizing agent. One such study by Morena and Salet [12] confirmed that in cardiac myocytes, the mitochondria were primary target sites for PDT. Recent studies demonstrated that in cells treated with several different photosensitizers, the interphase nucleus was the most sensitive target site, followed by the perinuclear cytoplasm, and finally the peripheral cytoplasm [13,14]. It was surprising to find such a high nuclear sensitivity because the highest level of sensitizer fluorescence was found in the cytoplasm around the nucleus. In addition, the vast majority of published cell studies have demonstrated that cellular phototoxicity is likely caused by the generation of reactive singlet oxygen by photosensitizers associated with organelles such as the lysosomes and mitochondria [15,16]. Notwithstanding this large body of literature, there are also several studies that demonstrate a PDT effect on DNA, chromosomes and the mitotic spindle (see the excellent review by Moan et al. [17]). However, it is not clear whether these effects are due to generation of singlet oxygen elsewhere in the cell, or directly at the nuclear/mitotic spindle site. The present investigation was undertaken to examine the possibility that the cell nucleus, and specifically the chromosomes, are primary target sites for PDT.

* Corresponding author. Tel.: +1-949-824-6996; fax: +1 949-824-8413; e-mail: mberns@bli.uci.edu

1011-1344/00/$ - see front matter
PII S1011-1344(00)00013-0

2. Materials and methods

2.1. Cell culture

PTK_2, Rat kangaroo (*Potorous tridactylis*) kidney cells, were used in this study. This cell line was originally obtained from American Type Culture Collection (ATCC) and is routinely grown as a monolayer in a modified Eagle's minimal essential medium with 10% fetal bovine serum. The cells were subcultured once a week into T-25 culture flask and maintained in a 37°C and 5–7% CO_2 incubator. The cells remain relatively flat throughout the cell cycle, permitting clear visualization of subcellular morphology and organelles, especially during mitosis.

Hep-2 cells from human larynx epidermoid carcinoma were originally obtained from the ATCC and grown as a monolayer in Eagle's minimum essential medium with 2 mM L-glutamine and Earle's BSS adjusted to contain 1.5 g/l sodium bicarbonate, 0.1 mM non-essential amino acids and 1.0 mM sodium pyruvate. The medium contained 10% fetal bovine serum. Hep-2 cells were used to confirm and extend the results obtained in the non-malignant mitotic PTK_2 cells.

Two and three days prior to the irradiation experiments, the cells were placed in a 35 mm Petri dish that had a 1.75 cm diameter hole in the middle, with a #1 grid-etched coverglass affixed over it. Twenty-four hours prior to laser microirradiation, the cells were placed in fresh culture medium containing 15 μg/ml (0.09 mM) 5-aminolevulinic acid (ALA). Cells without exposure to ALA served as controls. The Petri dishes were covered with aluminum foil immediately after treatment with ALA in order to shield the cells from ambient light. After 24 h of ALA treatment, individual healthy mitotic cells were identified under phase-contrast microscopy by visual observation. Each cell was identified by an alphabetic and digital coordinate on the gridded coverslip. Control non-ALA-exposed cells were also selected by this method.

2.2. Fluorescence microscopy

A Zeiss Axiovert inverted fluorescence microscope was used for fluorescence detection. Each individual cell was excited with UV light ($\lambda = 365$) using a 100 W arc lamp. Each cell was exposed to the UV light for 1 s. Individual fluorescence images was recorded for each selected cell using a cooled charge-coupled device (CCD, Princeton Instruments TE/CCD-576E/UV) and stored in IP Lab format in a Macintosh IIfx computer. A phase-contrast picture of each cell was also taken for reference. Images were digitally rendered (i.e., improving contrast, reducing background light) using IP Lab Spectrum.

2.3. Microirradiation of subcellular components

A laser microbeam system was used that employed an argon ion laser (Coherent Innova 90) pumped dye laser (Coherent 599 dye) to generate a 630 nm beam. The beam was directed through a Zeiss Axiovert inverted microscope using a Zeiss Neofluar 100× phase-contrast objective having a numerical aperture of 1.3. The focal-spot diameter was approximately 0.5 μm. For each PTK_2 cell, the laser beam was focused onto one of the following targets: (1) a chromosome; (2) the mitotic spindle; (3) the perispindle region; (4) the peripheral cytoplasm (random cytoplamic regions). For Hep-2 cells, chromosome and spindle regions were irradiated. Nuclei of interphase cells of both PTK_2 and Hep-2 were irradiated.

A Coherent (Palo Alto, CA) model 210 power meter was used to measure the power at the rear entrance to the objective. To determine the actual power reaching the irradiated sample, the dual-objective transmittance-measuring technique of Misawa et al. [18] was used. This method eliminates total internal reflection errors that are encountered in a direct objective-to-power measurement in air. Using this method, it was determined that each cell was exposed to 9 mW of power at a power of density 3.2×10^6 W/cm^2. The total energy densities per experiment were obtained by varying the exposure time. Total exposure time for ALA-treated cells varied from 3 to 60 s. Control cells were exposed for 180 s.

Immediately before laser irradiation of each cell, a phase-contrast image of the cell was obtained using the CCD camera. All pictures were stored using an IP Lab Spectrum software package. Each chamber was labeled and placed back into the CO_2 incubator after the irradiation. Each cell was relocated within 8 h and assayed for morphology and the ability to complete mitosis and form two daughter cells.

3. Results

3.1. Fluorescence detection

The fluorescence images of PTK_2 cells revealed no detectable autofluorescence in control untreated mitotic cells, though there were a few areas of non-specific fluorescence in adjacent non-mitotic cells. Fig. 1(A) is a phase-contrast image of an untreated control anaphase PTK_2 cell. Fig. 1(B) is a fluorescence image of the same cell. Fig. 1(C) is a phase-contrast image of a field of untreated control cells with a metaphase cell in the center. Fig. 1(D) is a fluorescence image of the same cells revealing no fluorescence in the metaphase cell and few areas of non-specific fluorescence in the non-mitotic cells.

Mitotic cells exposed to ALA exhibit very bright fluorescence throughout the whole cell except for the chromosomes, which exhibit little, if any, fluorescence. Fig. 2(A) is a phase-contrast image of ALA-treated cells with an anaphase cell in the center of the field. Fig. 2(B) is a fluorescence image of the same cells. Fig. 2(C) is a phase-contrast image of a field of ALA-treated cells with a metaphase cell in the center. Fig. 2(D) is the fluorescence image of the same cells. In inter-

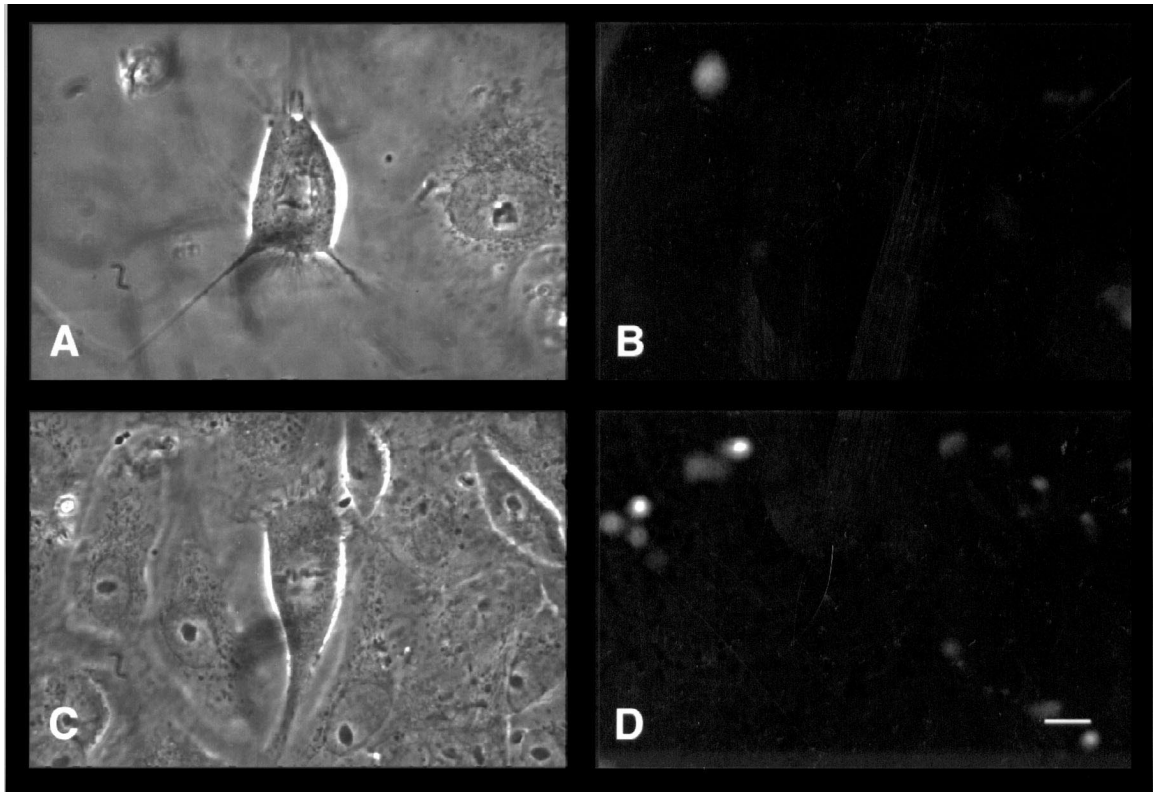

Fig. 1. Fluorescence images of control PTK2 mitotic cells: (A) phase-contrast image of a mitotic anaphase cell with neighboring interphase cells; (B) fluorescence image of the same cells; (C) phase-contrast image of a mitotic metaphase cell with neighboring interphase cells; (D) fluorescence image of the same cells. Bar scale, 10 μm.

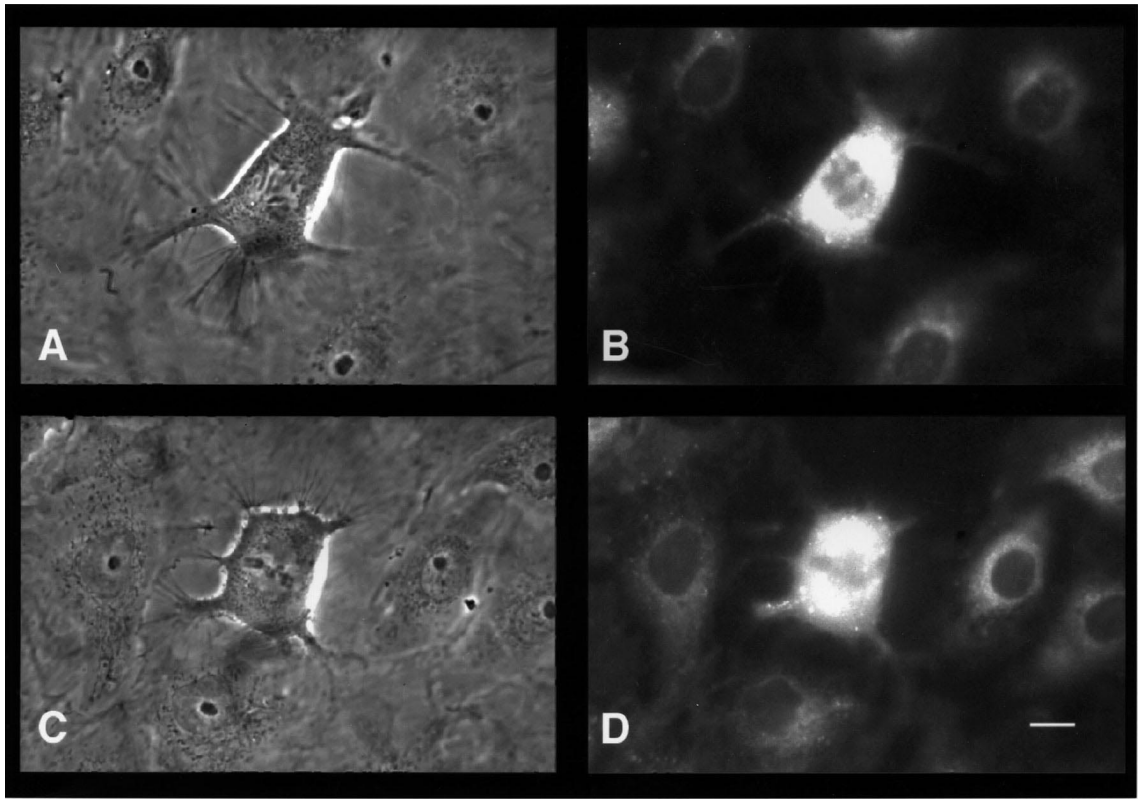

Fig. 2. Fluorescence images of ALA-treated PTK2 mitotic cells: (A) phase-contrast image of a mitotic anaphase cell with neighboring interphase cells; (B) fluorescence image of the same cells; (C) phase-contrast image of a mitotic metaphase cell with neighboring interphase cells; (D) fluorescence image of the same cells. Bar scale, 10 μm.

phase cells, fluorescence is strong in the perinuclear region and decreases peripherally.

In Hep-2 cells, similar fluorescence patterns were detected. There was no detectable autofluorescence in control cells (Fig. 3). In ALA-treated Hep-2 cells, the mitotic cells clearly exhibited brighter fluorescence than the interphase cells (Fig. 4). As in the PTK_2 cells, the chromosomes appear to exhibit no fluorescence.

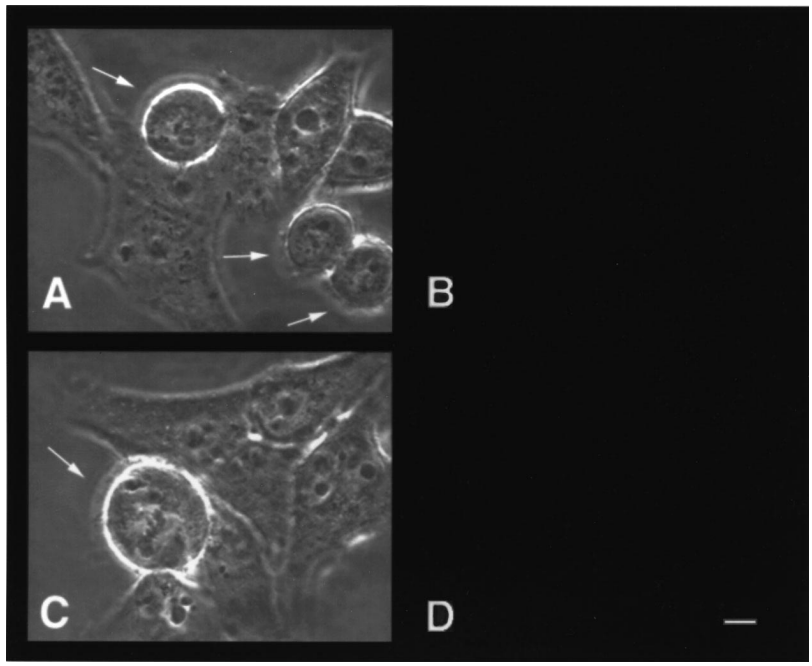

Fig. 3. Fluorescence images of control Hep-2 mitotic cells: (A) phase-contrast image of mitotic cells (arrow denotes) and interphase cells; (B) fluorescence image of the same cells; (C) phase-contrast image of a mitotic cell (arrow denotes) and interphase cells; (D) fluorescence image of the same cells. Bar scale, 10 μm.

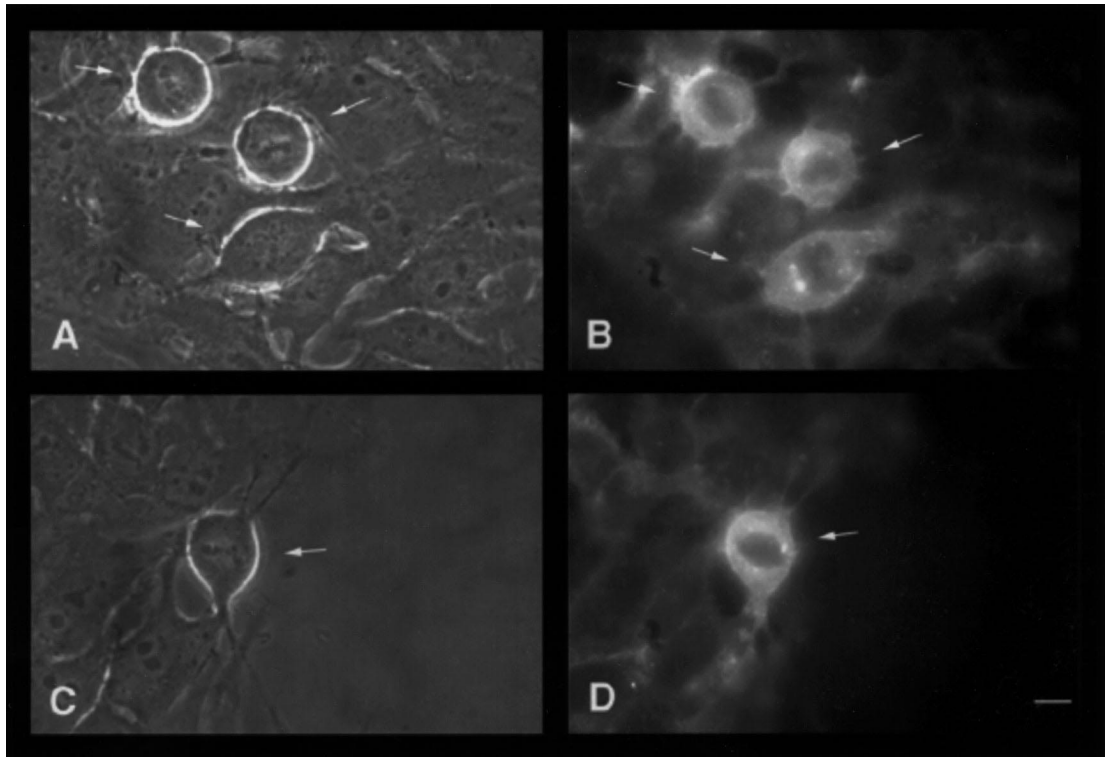

Fig. 4. Fluorescence images of ALA-treated Hep-2 mitotic cells: (A) phase-contrast image of three mitotic cells (arrows denote) with neighboring interphase cells; (B) fluorescence image of the same cells, with arrows denoting mitotic cells; (C) phase-contrast image of one mitotic cell (arrow denotes) with neighboring interphase cells; (D) fluorescence image of the same cells. Bar scale, 10 μm.

Statistics of relative fluorescence expressed in arbitrary units per pixel in PTK_2 and Hep-2 cells are presented in Table 1. After 24 h of ALA incubation, mitotic PTK_2 cells are three times more fluorescent than interphase cells ($p = 0.05$). In Hep-2, the mitotic cells are 2.2 times more fluorescent than interphase cells ($p = 0.01$).

3.2. Subcellular phototoxicity in mitotic cells

The total energy density (ED) delivered to the subcellular target area in PTK_2 cells was varied by changing the duration of laser exposure. The power parameters are listed in Table 2. A total of 299 mitotic PTK_2 cells in prophase, metaphase and anaphase were irradiated with the 0.5 μm diameter spot in the following subcellular regions: a chromosome, $n = 110$; spindle, $n = 66$; perispindle, $n = 60$; peripheral cytoplasm, $n = 63$. Seventy ALA-treated interphase cells were irradiated in their nuclear region to determine if there was a difference between the interphase and mitotic cells. An additional 16 control cells had chromosomes exposed to the laser but were not treated with ALA.

Each cell was followed for 8 to 24 h. Either two daughter cells were formed or the cells were blocked in mitosis and subsequent disintegration and lysis occurred. The data on irradiated cells are presented in Table 3 and the data for interphase cells are in Table 4. The comparative results demonstrate that the chromosome is the most sensitive target site followed by the perispindle region, the peripheral cytoplasm and spindle and, lastly, the interphase nucleus (Fig. 5).

Table 1
Fluorescence [a] comparison between mitotic and interphase cells

Group	Sample size	Mean	Maximum	Minimum	SD	Student's *t* value mitosis vs. interphase
PTK_2						
Mitosis	19	390	1352	46	424	2.435
Interphase	19	135	556	9	167	($p = 0.05$)
Hep-2						
Mitosis	19	571	861	202	210	5.244
Interphase	19	258	470	35	154	($p = 0.01$)

[a] Fluorescence expressed by arbitrary units per pixel.

Table 2
Power parameters used in laser microirradiation [a]

Time exposure (s)	Energy density ($\times 10^7$ J/cm^2)
60	19.2
30	9.6
20	6.4
15	3.2
10	3.2
5	1.6
3	1.0

[a] Power = 9 mW. Power density = 3.2×10^6 W/cm^2.

Table 3
Cell status 24 h after subcellular laser microirradiation in ALA-treated mitotic PTK_2 cells

Target of irradiation	Treatment with ALA	Time of exposure (s)	Total no. of cells	Damaged cells [a]	
				No.	%
Chromosome	−	180	16	0	0
	+	60	12	12	100
	+	30	8	7	87
	+	20	15	9	60
	+	15	10	4	40
	+	10	20	2	10
	+	5	9	1	11
	+	3	20	2	10
Spindle	+	60	10	7	70
	+	30	10	3	30
	+	20	12	2	17
	+	15	10	2	20
	+	10	19	2	11
	+	5	11	0	0
	+	3	10	0	0
Perispindle cytoplasm	+	60	10	8	80
	+	30	10	6	60
	+	20	10	5	50
	+	15	10	4	40
	+	10	10	3	30
	+	5	10	0	0
	+	3	10	0	0
Peripheral cytoplasm	+	60	10	6	60
	+	30	10	4	40
	+	20	10	3	30
	+	15	10	2	20
	+	10	13	2	15
	+	5	10	1	10
	+	3	10	0	0

[a] Cells were blocked in mitosis and disintegration and finally lysis followed.

Table 4
Cell status 24 h after laser microirradiation of interphase nucleus in ALA-treated PTK_2 cells

Time of exposure (s)	Total no. of cells attempted	Damaged cells [a]	
		No.	%
60	19	5	27
30	10	0	0
20	26	2	8
15	10	0	0
10	10	0	0

[a] Cells vacuolated, disintegrated and finally lysed.

Control mitotic cells without ALA treatment underwent mitosis and formed two daughter cells despite a laser dose three times that used in the experimental groups. Fig. 6(A) is an untreated control prophase PTK_2 cell just before laser microirradiation of the chromosome region. Fig. 6(B) is the same cell field after 4 h following 3 min of irradiation. Two normal daughter cells were produced. Fig. 6(C) is another untreated control mitotic cell (anaphase) before chromosome irradiation. Fig. 6(D) is at the same cell field 4 h later, after

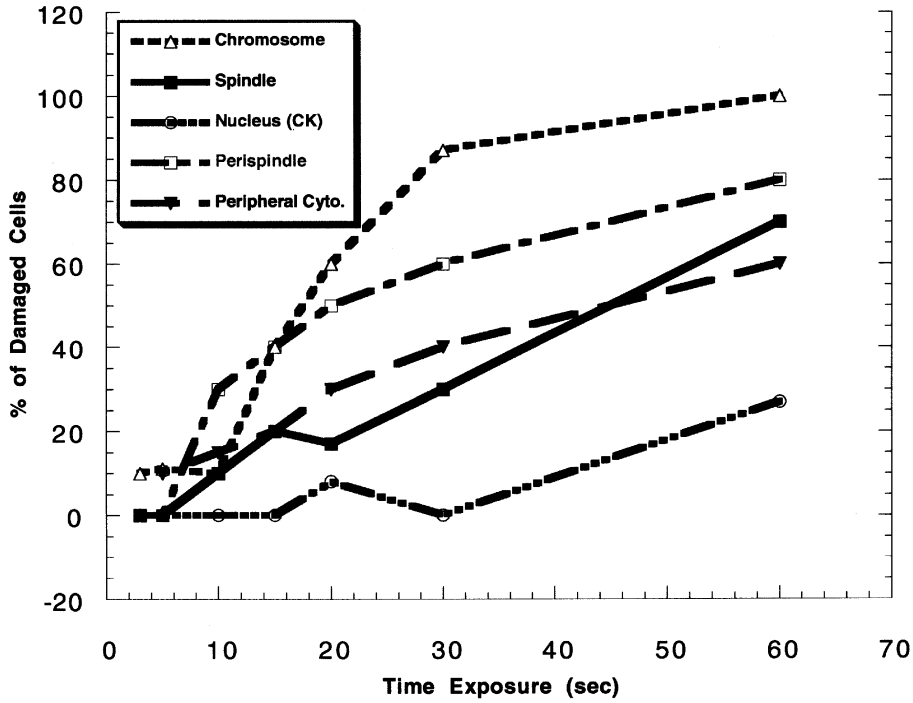

Fig. 5. Cellular toxicity at 24 h after subcellular laser microirradiation in PTK_2 cells treated with ALA.

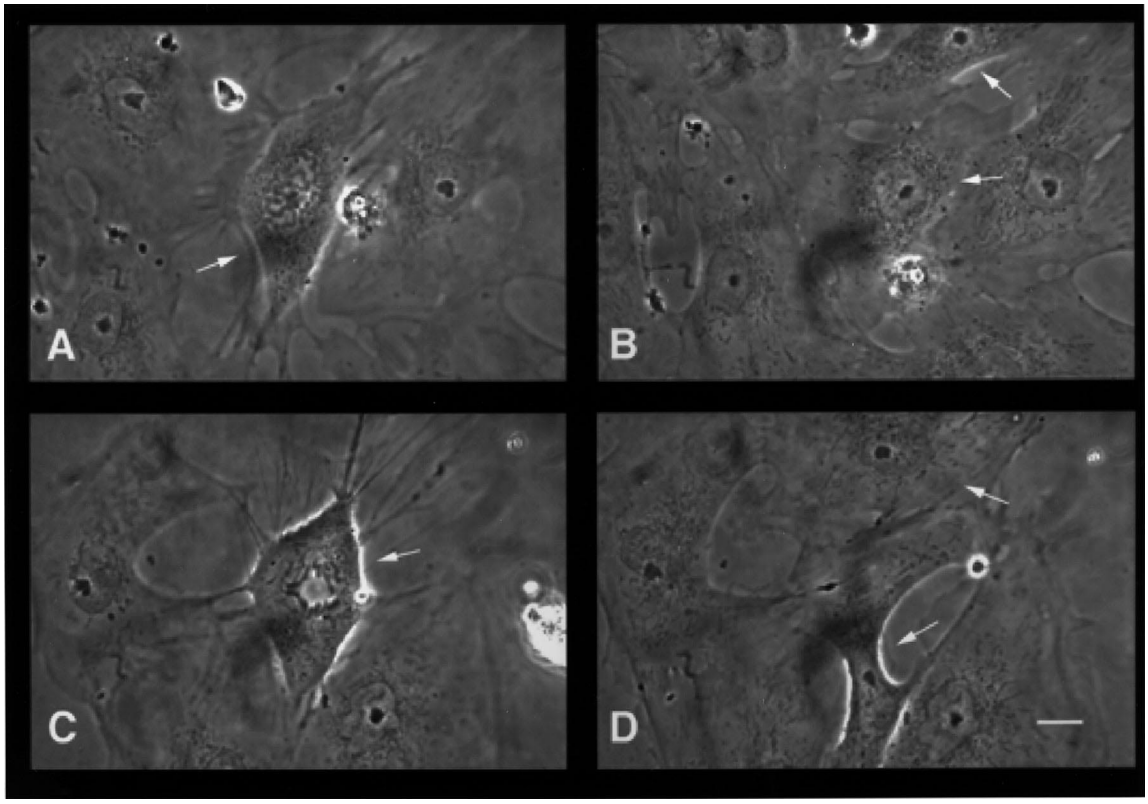

Fig. 6. Cellular status at 4 h after a 3 min laser microirradiation of chromosome in control PTK_2 mitotic cells (A) phase-contrast image of a prophase cell (arrow denotes) just prior to irradiation; (B) two daughter cells (arrows denote) formed post irradiation; (C) phase-contrast image of an anaphase cell (arrow denotes) just prior to irradiation; (D) two daughter cells (arrows denote) formed post irradiation. Bar scale: 10 μm.

Table 5
Cell status 8 h after subcellular laser microirradiation in ALA-treated mitotic Hep-2 cells

Target of irradiation	Treatment with ALA	Time of exposure (s)	Total no. of cells	Damaged cells [a]	
				No.	%
Chromosome	−	120	15	2	13
	−	60	14	1	7
	+	60	10	10	100
	+	30	13	8	61
	+	20	15	6	44
	+	10	10	3	30
	+	5	10	1	10
	+	3	17	1	6
Spindle	+	60	13	11	85
	+	30	15	6	40
	+	20	10	3	30
	+	10	15	1	7
	+	15	13	1	8
	+	3	12	0	0
Nucleus (interphase)	+	60	9	6	67
	+	30	9	3	33
	+	20	16	3	19
	+	10	19	2	11
	+	5	16	1	7
	+	3	15	0	0

[a] Cells were blocked in mitosis, disintegrated or lysed.

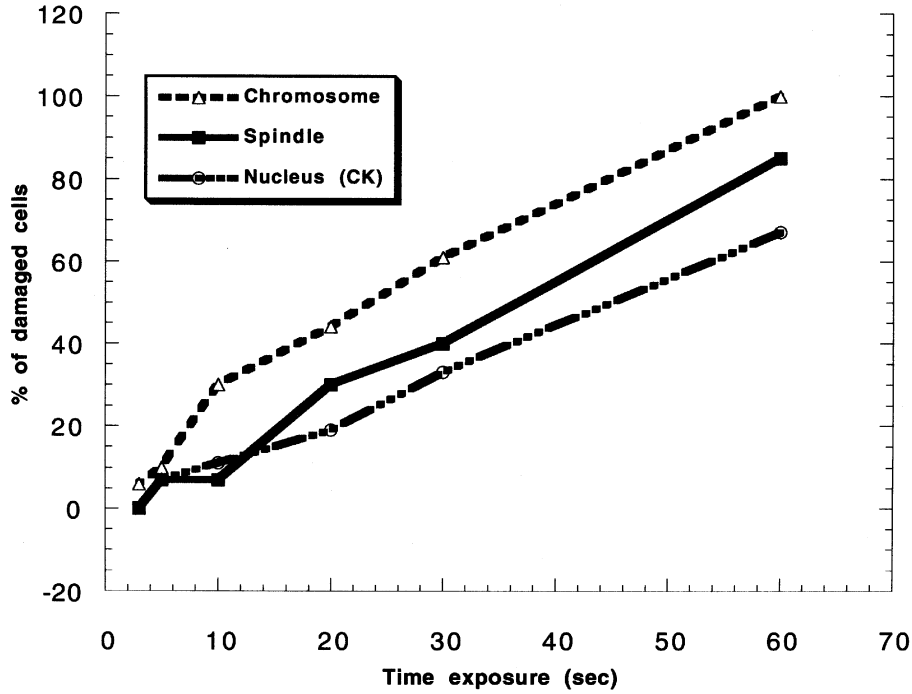

Fig. 7. Cellular toxicity at 5 h after subcellular laser microirradiation in Hep-2 cells treated with ALA.

3 min of irradiation. Mitosis was completed with two daughter cells of normal appearance being formed.

A total of 153 Hep-2 mitotic cells were irradiated in the following regions: a chromosome, $n=75$; spindle, $n=78$. Eighty-four ALA-treated interphase cells were irradiated in their nuclear region for comparison. Data of Hep-2 cells are presented in Table 5 and summarized in Fig. 7. The chromosome is the most sensitive target site, followed by the spindle, and, lastly, the interphase nucleus.

3.3. Differential sensitivity of various cell regions: cell morphology

Fig. 8 presents the cell status before and after laser irradiation of two mitotic PTK_2 cells. Fig. 8(A) is a metaphase

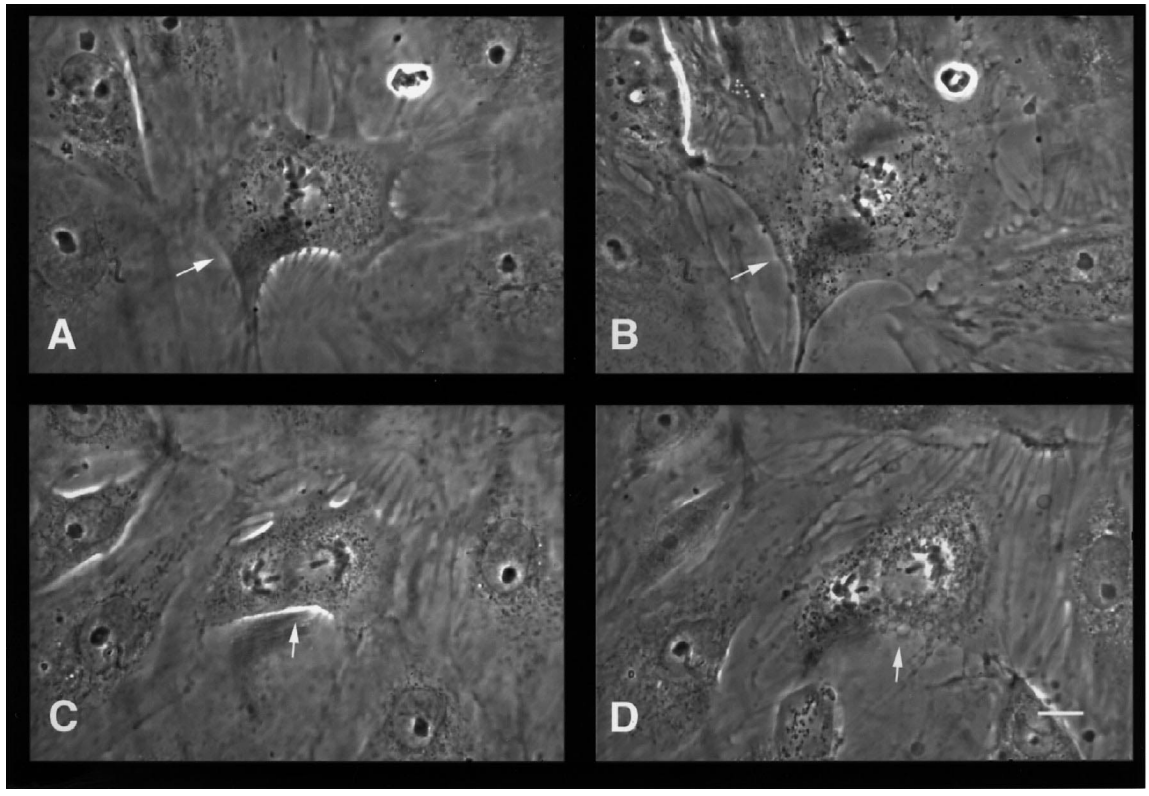

Fig. 8. Cellular damage at 4 h after a 1 min laser microirradiation of the chromosome area in ALA-treated mitotic PTK_2 cells (A) phase-contrast image of a metaphase cell (arrow denotes) just prior to irradiation; (B) the same cell post irradiation, mitotic event stalled and the cell (arrow denotes) starts to disintegrate; (C) phase-contrast image of an anaphase cell (arrow denotes) just prior to irradiation; (D) the same cell (arrow denotes) post irradiation, mitotic event stalled and the cell starts to disintegrate. Bar scale, 10 μm.

cell pretreated with ALA for 24 h just prior to irradiation of a single chromosome site. Fig. 8(B) is the same cell 4 h post irradiation. Fig. 8(C) and Fig. 8(D) show an anaphase cell before and after 60 s of laser microirradiation of a single chromosome region. Within 24 h post irradiation, cytoplasmic disintegration and lysis occur. Irradiation of chromosomes results in the inhibition of the ongoing mitotic event.

Fig. 9 presents the cell status before and after laser irradiation of two mitotic Hep-2 cells. Fig. 9(A) is a mitotic cell pretreated with ALA for 24 h prior to irradiation of a single chromosome site. Fig. 9(B) is the same cell 3 h after a 1 min irradiation. Fig. 9(C) and Fig. 9(D) show another Hep-2 cell before and 3 h after a 1 min laser irradiation. As in PTK_2 cells, laser exposure resulted in blocking of the ongoing mitosis.

4. Discussion

Under the irradiation conditions used in this study, it appears that the chromosomes of ALA-treated cells are the most light-sensitive subcellular target when compared with the nucleoplasm, mitotic spindle and the cytoplasm. This observation is consistent with previous studies demonstrating that the interphase nuclei of cells treated with ALA, Photofrin and Lutetium Texaphyrin were more light sensitive than other cell regions [13,14]. However, those studies were on interphase cells. In the present study, the nuclear sensitivity appears to be attributed to a direct effect on the chromosomes. The fact that the interphase nucleus is less sensitive than the mitotic chromosomes as well as any of the other three regions of the mitotic cell (Figs. 6 and 8, Tables 3–5) may be due to several reasons. First, the chromatin of the mitotic cell is highly condensed as compared with that of the interphase nucleus. Thus, any sensitizer associated with the chromatin will be more concentrated in the mitotic chromosome. Secondly, the mitotic cell may convert more ALA to the active photosensitizer, Protoporphyrin IX, than the interphase cell. Thirdly, more ALA may enter the mitotic cell than the interphase cell.

The fluorescent images confirm that there is two to three times as much Protoporphyrin IX in the mitotic cells as in the surrounding interphase cells (Table 1, Fig. 2(B) and (D) and Fig. 4(B) and (D)). This increase in fluorescence is not due to a higher concentration of fluorophore per unit volume as a result of the cell rounding up in mitosis, because PTK_2 cells remain flat throughout mitosis. However, this increase could be due to either more ALA in the cell and thus more Protoporphyrin IX, or a higher conversion efficiency of ALA to Protoporphyrin IX. As noted previously [13,14], the most sensitive region of the cell has the least amount of detectable fluorescence. The same observation is made in the present study: the chromosomes are the most sensitive targets and no

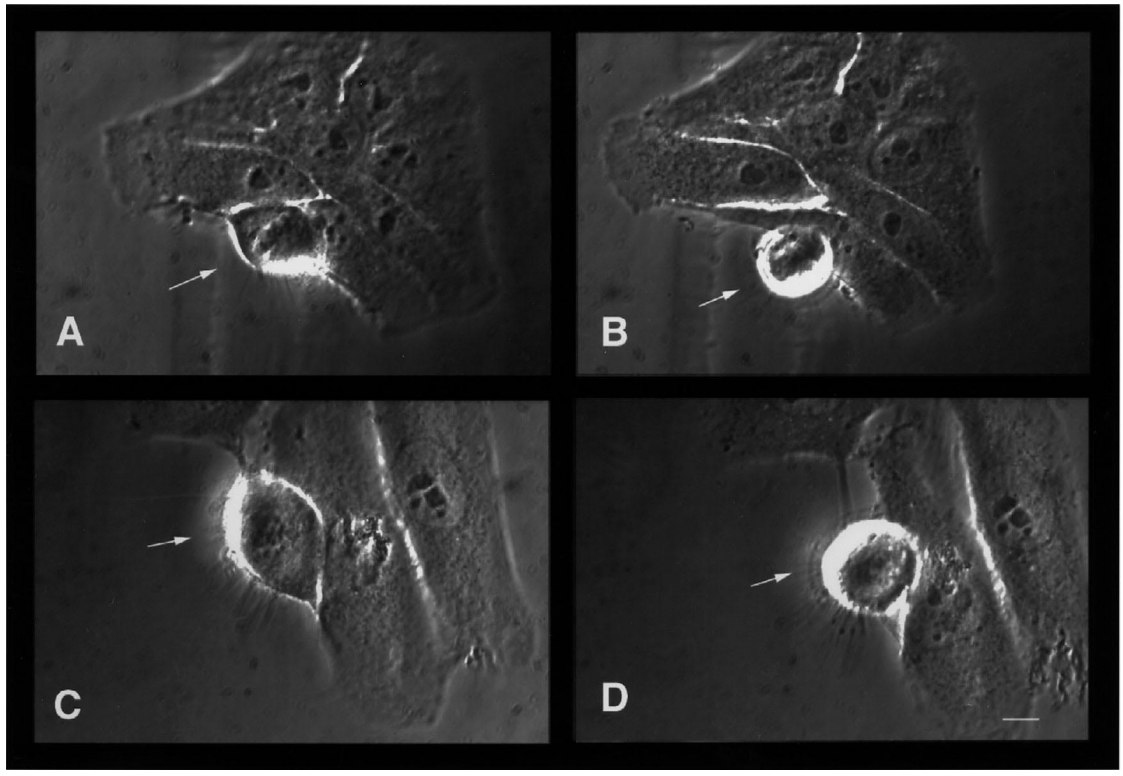

Fig. 9. Cellular damage at 3 h after a 1 min laser microirradiation of the chromosome region in ALA-treated mitotic Hep-2 cells (A) phase-contrast image of a mitotic cell (arrow denotes) just prior to irradiation; (B) the same cell (arrow denotes) post irradiation, mitotic event blocked and the cell rounded up; (C) phase-contrast image of another mitotic cell (arrow denotes) just prior to irradiation; (D) the same cell (arrow denotes) post irradiation, mitotic event blocked, and the cell rounded up.

fluorescence can be detected with the sensitive cooled CCD system. This observation may be explained either by the fact that the amount of Protoporphyrin IX bound to the chromosomes is below the level of the fluorescence detection system, or that almost all of the absorbed photon energy generates photochemistry as opposed to fluorescence. This would occur if the excited triplet state of Protophorphrin IX has a higher probability of interacting with molecular oxygen to produce singlet oxygen as opposed to the excited Protophorphrin IX giving up its energy via fluorescence.

Generally, the mechanism of PDT at the cellular level is thought to be generation of singlet oxygen in association with membrane-rich cytoplasm organelles such as mitochondria [15] and lysosomes [16]. There have been several studies examining possible PDT effects on the nucleus, cell division and the cytoskeleton [17,19–22]. In a rather comprehensive review, Moan et al. [17] point out that the photosensitizers used in PDT generally do not bind to DNA and do not produce damage in the dark. However, it is noted that exposure to light does result in sister chromatid exchanges [21,22] DNA–protein crosslinking, [23] and DNA single-strand breaks [22]. In addition, there is some evidence that microtubule assembly [20] and the organization of the mitotic apparatus [19] are affected by PDT. However, in all of these studies, there is no evidence of direct binding of the photosensitizer to the DNA, chromatin or the mitotic apparatus. The results could be due to generation of singlet oxygen at a nearby site with subsequent effects on the DNA and microtubules. Our results suggest a more direct effect on the chromosomes.

In addition to the chromosome-specific nature of PDT, the present study also demonstrates that the mitotic cell may be more sensitive to PDT because of either an increase in photosensitizer uptake, or in the case of ALA, a higher conversion rate of ALA to Protoporphyrin IX. Recently it has been shown by Wyld et al. that the uptake and efficiency of PDT are cell-cycle dependent [24]. These authors demonstrated that cells in the mitotic phase of the cell cycle were more susceptible to PDT than cells in the G or S phases.

In conclusion, this study suggests a potential direct effect on photodynamic sensitization on the chromosomes of cells. However, care must be taken in extrapolating these data because the amounts of light per volume used in these laser microbeam studies are orders of magnitude greater than those used in whole-cell or in vivo studies. Nonetheless, selective sensitivity of the chromosomes under the conditions used in these studies is strongly supported because of the lack of sensitivity of the non-drug-treated controls, as well as the reduced sensitivity of the other cell regions. Though we cannot be sure which organelles were contained in the perispindle cytoplasm or peripheral cytoplasm for any single exposure, the number of replicates of each experiment, the random nature of the cellular spot selected for irradiation, and the increase in cell damage as a function of total dose (Table 3)

would all suggest that there were sensitive organelle structures within these cell regions. The chromosomes appeared to be the most sensitive subcellular target.

Acknowledgements

This work was supported by the following grants: NIH, contract numbers 2R01CA32248 and RR01192; Office of Naval Research, contract number ONR N00014-91-C-0134; Department of Energy, contract number DE-FG03-91ER 61227; Beckman Laser Institute Endowment.

References

[1] T.J. Dougherty, Photodynamic therapy, Photochem. Photobiol. 58 (1993) 895–900.
[2] A.M.R. Fisher, A.L. Murphee, C.J. Gomer, Clinical and preclinical photodynamic therapy, Lasers Surg. Med. 17 (1995) 2–31.
[3] R.A. Steiner, Y. Tadir, B.J. Tromberg, T. Krasieva, A.T. Ghazains, P. Wyss, M.W. Berns, Photosensitization of the rat endometrium following 5-aminolaevulinic acid induced photodynamic therapy, Lasers Surg. Med. 18 (1996) 301–308.
[4] U. Schmidt-Erfurth, J. Miller, M. Sickenberg, A. Bunse, H. Laqua, E. Gragoudas, L. Zografos, R. Birngruber, H. van dan Bergh, A. Strong, J. Manjuris, M. Fsadni, A.M. Lane, B. Piguet, N.M. Bressler, Photodynamic therapy of subfoveal choroidal neovascularization: clinical and angiographic examples, Grafes Arch. Clin. Exp. Ophthalmol. 236 (1998) 365–374.
[5] S.C. Lin, C.P. Lin, J.R. Feld, J.S. Daker, C.A. Puliafito, The photodynamic occlusion of chorodial vessels using benzoporphyrin derivative, Current Eye Research. 13 (1994) 513–522.
[6] A. Orenstein, J.S. Nelson, L.H. Liaw, R. Kaplan, S. Kimel, M.W. Berns, Photochemotherapy of hypervascular dermal lesions: a possible alternative to photothermal therapy, Lasers Surg. Med. 19 (1990) 334–343.
[7] M.W. Berns, M. Rettenmaier, J. McCullough, Response of psoriasis to red laser light (630 nm) following systemic injection of hematoporphyrin derivative, Lasers Surg. Med. 4 (1984) 73–77.
[8] W.H. Boehncke, W. Sterry, R. Kaufmann, Treatment of psoriasis by topical photodynamic therapy with polychromatic light, Lancet 343 (1994) 801.
[9] G.M. Vincent, R.W. Mackie, E. Orme, J. Fox, M. Johnson, In vivo photosensitizer enhanced laser angioplasty in atheroscleorotic miniswine, J. Clin. Laser Med. Surg. 8 (1990) 59–61.
[10] P.C. Dartsch, T. Ischinger, E. Betz, Differential effect of Photofrin-II on growth of human smooth muscle cells from nonatherosclerotic arteries and atheromatous plaques in vitro, Arteriosclerosis 10 (1990) 616–624.
[11] T.J. Dougherty, C.J. Gomer, B.W. Henderson, G. Jori, D. Kessel, M. Korbelik, J. Moan, Q. Peng, Photodynamic therapy, J. Natl Cancer Inst. 90 (1998) 889–905.
[12] G. Moreno, C. Salet, Cytotoxic effects following micro-irradiation of cultured cells sensitized with haematoporphyrin derivative, Int. J. Radiat. Biol. 47 (1985) 383–386.
[13] H. Liang, D.S. Shin, Y.E. Lee, D. C Nguyen, T.C. Trang, A.W. Pan, S.L.J. Huang., D.H. Chong, M.W. Berns, Subcellular phototoxicity of 5-aminolaevulinic acid (ALA), Lasers Surg. Med. 22 (1998) 14–24.
[14] H. Liang, D.S. Shin, Y.E. Lee, D.C. Nguyen, S. Kasravi, T. Do, P. Aurasteh, M.W. Berns, Subcellular phototoxicity of Photofrin-II and lutetium texaphyrin in cells in vitro, Lasers Med. Sci., in press.
[15] M.W. Berns, A. Dahlman, F.M. Johnson, R. Burns, D. Sperling, M. Guiltinan, A. Siemans, R. Walter, W. Wright, M. Hammer-Wilson, A. Wile, In vitro cellular effects of hematoporphyrin derivative, Cancer Res. 42 (1982) 2326–2329.
[16] C.J. Gomer, N. Rucker, A. Ferrario, S. Wong, Properties and applications of photodynamic therapy, Radiat. Res. 120 (1989) 1–18.
[17] J. Moan, K. Berg, E. Kvam, Effects of Photodynamic treatment on DNA and DNA-related cell functions, in: D. Kessel (Ed.), Photodynamic Therapy of Neoplastic Disease, vol. 1, CRC Press, Boca Raton, FL, 1990, Ch. 12, pp. 197–209.
[18] H. Misawa, M. Koshioka, K. Sasaki, N. Kitamura, H. Masuhara, Three dimensional optical trapping and laser ablation of a single polymer latex particle in water, J. Appl. Phys. 60 (1991) 1052–1057.
[19] K. Berg, J. Moan, Photodynamic effects of Photofrin II on cell division in human NHIK 3025 cells, Int. J. Radiat. Biol. 53 (1988) 797–811.
[20] K. Berg, J. Moan, J.C. Bommer, J.W. Winkelman, Cellular inhibition of microtubule assembly by photoactivated sulphonated *meso*-tetraphenylporphines, Int. J. Radiat. Biol. 58 (1990) 475–487.
[21] C. Gomer, N. Rucker, A. Banerjee, W.F. Benedict, Comparison of mutagenicity and induction of sister chromatid exchange in Chinese hamster cells exposed to hematoporphyrin derivative photoradiation, ionizing radiation or ultraviolet radation, Cancer Res. 43 (1983) 2622–2627.
[22] J. Moan, H. Waksvik, T. Christensen, DNA single-strand breaks and sister chromatid exchanges induced by treatment with hematoporphyrin and light or by X-rays in human NHK 3025 cells, Cancer Res. 40 (1980) 2915–2918.
[23] T. Dubbelman, A.-R vanSteveninck, J. vanSteveninck, Hematoporphyrin-induced photo-oxidation and photodynamics crosslinking of nucleic acids and their constituents, Biochim. Biophys. Acta 719 (1982) 47–52.
[24] L. Wyld, O. Smith, J. Lawry, M.W. Reed, N.J. Brown, Cell cycle phase influences tumor cell sensitivity to aminolaevulinic acid-induced photodynamic therapy in vitro, Br. J. Cancer 78 (1998) 50–55.